Chemical Engineering Journal 165 (2010) 883–890

Contents lists available at ScienceDirect

Chemical Engineering Journal

journal homepage: www.elsevier.com/locate/cej

Optimization of preparation conditions for mangosteen peel-based activated carbons for the removal of Remazol Brilliant Blue R using response surface methodology

Mohd Azmier Ahmad*, Rasyidah Alrozi

School of Chemical Engineering, Engineering Campus, Universiti Sains Malaysia, 14300 Nibong Tebal, Penang, Malaysia

ARTICLE INFO

Article history:
Received 2 September 2010
Received in revised form 18 October 2010
Accepted 18 October 2010

Keywords:
Mangosteen peel
Activated carbon
Remazol Brilliant Blue R
Central composite design
Optimization

ABSTRACT

This study investigates the optimal conditions for preparation of activated carbons from mangosteen peel (MP) for removal of Remazol Brilliant Blue R (RBBR) reactive dye from aqueous solution. The MP activated carbon was prepared using physiochemical activation method which consisted of potassium hydroxide (KOH) treatment and carbon dioxide (CO_2) gasification. Central composite design (CCD) was used to determine the effects of the three preparation variables; CO_2 activation temperature, CO_2 activation time and KOH impregnation ratio (IR) on RBBR percentage removal and activated carbon yield. Based on the CCD, a quadratic model and a two-factor interaction (2FI) model were respectively developed for RBBR percentage removal and carbon yield. The significant factors on each experimental design response were identified from the analysis of variance (ANOVA). The optimum conditions for MP activated carbon preparation were obtained by using activation temperature of 828 °C, activation time of 1 h and IR of 3.0, which resulted in 80.35% of RBBR removal and 20.76% of activated carbon yield.

1. Introduction

Almost 45% of textile dyes produced worldwide belongs to the reactive class [1]. Reactive dyes are common dyes used for dyeing cellulosic fibres due to their favorable characteristics of bright color, water-fastness, simple application techniques and low energy consumption [2]. They are usually characterized by nitrogen to nitrogen double bonds (N=N azo bonds) where the color of azo dyes is due to this azo bond and the associated chromophores [3]. The formation of a covalent bond between the dye molecule and the fibre is much stronger than the physio-chemical bond between other classes of dyes and cellulose [4]. However, reactive dyes pose the greatest problem in textiles wastewater since they are not easily biodegradable, and thus color may still remain in the effluent [5]. In fact, the expanded uses of azo dyes and their reaction products such as aromatic amines are highly carcinogenic. The discharge of these wastewaters into receiving streams causes damage not only to aquatic life but also to human beings [6].

In recent years, many processes have been applied for the treatment of reactive dyes from wastewater including biological, physical and chemical process [7]. Among them, adsorption process with activated carbon has been proved to be superior compared to other techniques in terms of its simplicity of design, high efficiency and ease of operation [8]. However, the manufacturing costs of commercial activated carbons are in fact rather high. As such, there is a need to produce activated carbon with high adsorption performance from alternative material that is cheaper and readily available. From the literature, many studies have been carried out to prepare low cost activated carbons from agricultural wastes such as sugar beet pulp [2], bamboo [5], pomegranate peel [8], date stone [9], vetiver roots [10], corn grain [11], cotton stalk fibre [12], oil palm empty fruit bunch [13], coconut husk [14] and rice straw [15].

In this work, an attempt was made in preparing activated carbon from mangosteen peel (MP) precursor. Mangosteen (*Garcinia mangostana* L.), a tropical evergreen tree has been planted in Malaysia with the total acreage between 7000 and 8000 ha [16]. It is also being planted in other countries such as India, Thailand, Vietnam and Philippines. This fruit has become an economically important species since the demand in the domestic and export markets are tremendous. However, due to the high consumption of mangosteen's edible part, massive amounts of the peels are disposed, causing a severe problem in the community as they gradually ferment and release off odours [17]. Therefore, by utilizing MP into activated carbon will decrease the cost of wastes disposal and also converted this waste into value-added product [18].

Currently no study has been done on optimization of the production of activated carbon from MP using the response surface methodology (RSM) approach. RSM has been found to be a useful

* Corresponding author. Tel.: +60 4 5996459; fax: +60 4 5941013.
E-mail addresses: chazmier@eng.usm.my, chazmier@hotmail.com (M.A. Ahmad).

1385-8947/$ – see front matter © 2010 Elsevier B.V. All rights reserved.
doi:10.1016/j.cej.2010.10.049

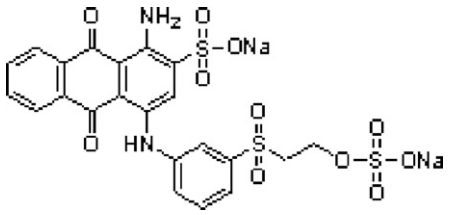

Fig. 1. Chemical structure of RBBR dye.

tool to study the interactions of two or more factors [19]. A standard RSM design called a central composite design (CCD) is suitable for fitting a quadratic surface and it helps to optimize the effective parameters with a minimum number of experiments, as well as to analyze the interaction between the parameters [20]. RSM has just recently been used for the optimization of activated carbon production from rattan sawdust [19], Tamarind wood [21] and Turkish lignite [22] by chemical activation whereas oil palm empty fruit bunch [13] and coconut husk [14] by physiochemical activation method. The goal of this work was to optimize the preparation conditions of activated carbon from MP for the removal of Remazol Brilliant Blue R (RBBR) dye. The effects of preparation variables; activation temperature, activation time and chemical impregnation ratio were studied simultaneously to obtain a high activated carbon yield and high RBBR percentage removal from aqueous solution using the CCD.

2. Materials and methods

2.1. Adsorbate

Remazol Brilliant Blue R (RBBR) supplied by Sigma–Aldrich (M) Sdn Bhd, Malaysia was used as an adsorbate. Deionized water was used to prepare all solutions. RBBR has a chemical formula of $C_{22}H_{16}N_2Na_2O_{11}S_3$ with molecular weight of 626.54 g mol^{-1}. The chemical structure of RBBR is shown in Fig. 1.

2.2. Preparation of activated carbon

Mangosteen peel (MP) used for preparation of activated carbon was obtained from the local market in Nibong Tebal, Penang, Malaysia. MP was firstly washed with water and subsequently dried at 105 °C for 24 h to remove the moisture contents. The dried MP was ground and sieved to the size of 1–2 mm before loaded in a stainless steel vertical tubular reactor placed in a tube furnace. Carbonization step was carried out at 700 °C for 2 h under purified nitrogen (99.99%) flow at flowrate of 150 ml min^{-1}. The char produced was mixed with KOH pellets with different impregnation ratio (IR), as calculated using following equation:

$$\mathrm{IR} = \frac{w_{\mathrm{KOH}}}{w_{\mathrm{char}}} \quad (1)$$

where w_{KOH} is the dry weight of KOH pellets (g) and w_{char} is the dry weight of char (g). Deionized water was then added to dissolve all the KOH pellets.

The mixture was then dehydrated in an oven at 105 °C for 24 h to remove moisture. The activation step was done using similar reactor as in carbonization step. Once the final activation temperature was reached, the gas flow was switched from nitrogen to CO_2 at flowrate of 150 ml min^{-1} for different period of time. The activated product was then cooled to room temperature under nitrogen flow. Then, the sample was washed with hot deionized water and HCl (0.1 M) until the pH of the washed solution reached 6.5–7.

2.3. Adsorption studies

For batch adsorption studies, 300 mg of adsorbent were mixed with 200 ml aqueous dye solutions of 100 mg/l initial concentration in 20 sets of 250 ml Erlenmeyer flasks. The mixture was agitated at 120 rpm at 30 °C until equilibrium was reached. The pH of the solution was natural without any pH adjustment. The concentration of RBBR dye solution was determined using a double UV–vis spectrophotometer (UV-1800 Shimadzu, Japan) at maximum wavelength of 590 nm. The percentage removal at equilibrium was calculated by the following equation:

$$\text{Removal}\ (\%) = \frac{(C_o - C_e)}{C_o} \times 100 \quad (2)$$

where C_o and C_e are the liquid-phase dye concentrations at initial state and at equilibrium (mg/l), respectively.

2.4. Activated carbon yield

The activated carbon yield was calculated based on the following equation:

$$\text{Yield}\ (\%) = \frac{w_c}{w_o} \times 100 \quad (3)$$

where w_c and w_o are the dry weight of final activated carbon (g) and the dry weight of precursor (g), respectively.

2.5. Design of experiments

RSM is a collection of statistical and mathematical techniques that uses quantitative data from appropriate experiments to determine regression model equations and operating conditions which are useful for developing, improving and optimizing processes [13]. In this work, a standard RSM design, known as central composite design (CCD) was applied to study the variables for preparing the activated carbons from MP. This method can reduce the number of experimental trials needed to evaluate multiple parameters and their interactions [14]. Generally, the CCD consists of 2^n factorial runs, $2(n)$ axial runs and six center runs, where n is the number of factors.

In the present study, the activated carbons were prepared using physiochemical activation method where the variables studied were CO_2 activation temperature (x_1), CO_2 activation time (x_2) and KOH:char IR (x_3). These three variables together with their respective ranges were chosen based on the literature and preliminary studies as given in Table 1. For each categorical variable, a 2^3 full factorial CCD for the three variables, consisting of 8 factorial points, 6 axial points and 6 replicates at the center points were employed, indicating that altogether 20 experiments for this procedure for

Table 1
Independent variables and their coded levels for the central composite design.

Variables (factors)	Code	Units	Coded variable levels				
			$-\alpha$	−1	0	+1	$+\alpha$
Activation temperature	x_1	°C	648.87	700.00	775.00	850.00	901.13
Activation time	x_2	h	0.32	1.00	2.00	3.00	3.68
Impregnation ratio (IR)	x_3	–	0.15	1.00	2.25	3.50	4.35

Table 2
Experimental design matrix for preparation of MP activated carbons.

Run	Level			Activated carbon preparation variable			RBBR removal, Y_1 (%)	Activated carbon yield, Y_2 (%)
				Activation temperature, x_1 (°C)	Activation time, x_2 (h)	IR, x_3		
1	−1	−1	−1	700.00	1.00	1.00	37.47	25.34
2	+1	−1	−1	850.00	1.00	1.00	39.15	21.05
3	−1	+1	−1	700.00	3.00	1.00	36.65	24.45
4	+1	+1	−1	850.00	3.00	1.00	39.51	12.56
5	−1	−1	+1	700.00	1.00	3.50	60.43	19.57
6	+1	−1	+1	850.00	1.00	3.50	83.56	19.09
7	−1	+1	+1	700.00	3.00	3.50	61.53	19.31
8	+1	+1	+1	850.00	3.00	3.50	82.20	11.38
9	−1.682	0	0	648.87	2.00	2.25	30.54	23.72
10	+1.682	0	0	901.13	2.00	2.25	80.54	17.56
11	0	−1.682	0	775.00	0.32	2.25	64.89	25.51
12	0	+1.682	0	775.00	3.68	2.25	73.49	19.84
13	0	0	−1.682	775.00	2.00	0.15	35.05	26.59
14	0	0	+1.682	775.00	2.00	4.35	79.53	19.56
15	0	0	0	775.00	2.00	2.25	76.45	21.31
16	0	0	0	775.00	2.00	2.25	77.54	20.18
17	0	0	0	775.00	2.00	2.25	77.83	20.75
18	0	0	0	775.00	2.00	2.25	77.55	21.01
19	0	0	0	775.00	2.00	2.25	76.54	20.02
20	0	0	0	775.00	2.00	2.25	77.40	20.11

each precursor, as calculated from Eq. (4) [20]:

$$N = 2^n + 2n + n_c = 2^3 + 2(3) + 6 = 20 \quad (4)$$

where N is the total number of experiments required.

The center points are used to determine the experimental error and the reproducibility of the data. The axial points are located at ($\pm\alpha$, 0, 0), (0, $\pm\alpha$, 0) and (0, 0, $\pm\alpha$) where α is the distance of the axial point from center and makes the design rotatable. In this study, α value was fixed at 1.682 (rotatable). The experimental sequence was randomized in order to minimize the effects of the uncontrolled factor. The two responses were RBBR removal (Y_1) and activated carbon yield (Y_2). Each response was used to develop an empirical model which correlated the response to the three activated carbon preparation variables using a second-degree polynomial equation as given by Eq. (5):

$$Y = b_o + \sum_{i=1}^{n} b_i x_i + \left(\sum_{i=1}^{n} b_{ii} x_i \right) + \sum_{i=1}^{n-1} \sum_{j=i+1}^{n} b_{ij} x_i x_j \quad (5)$$

where Y is the predicted response, b_o the constant coefficient, b_i the linear coefficients, b_{ij} the interaction coefficients, b_{ii} the quadratic coefficients and x_i, x_j are the coded values of the activated carbon preparation variables.

2.6. Model fitting and statistical analysis

The experimental data were analyzed using a statistical software Design Expert software version 6.0.6 (STAT-EASE Inc., Minneapolis, USA) for regression analysis to fit the second-degree polynomial equation and also for the evaluation of the statistical significance of the equations developed.

2.7. Characterization of activated carbon

The surface area, pore volume and average pore diameter of the MP activated carbon prepared under optimum preparation conditions were determined by using Micromeritics ASAP 2020 volumetric adsorption analyzer. Prior to analysis, the sample was degassed for 2 h under vacuum at 300 °C. After degassing, the sample was transferred to the analysis system where it was cooled in liquid nitrogen. A 21-point analysis was carried out at 77 K to obtain the nitrogen adsorption isotherm. The surface area of the sample was determined using Brunauer–Emmett–Teller (BET) equation. The total pore volume was estimated to be the liquid volume of nitrogen at a relative pressure of 0.98.

The surface morphology of the samples was examined using a scanning electron microscope (JEOL, JSM-6460 LV, Japan). Proximate analysis was carried out using thermogravimetric analyser (Perkin Elmer TGA7, USA) and elemental analysis was performed using Elemental Analyzer (Perkin Elmer Series II 2400, USA).

3. Results and discussion

3.1. Development of regression model equation

CCD was used to develop a polynomial regression equation in order to analyze the correlation between the activated carbon preparation variables to the RBBR removal and activated carbon yield. Table 2 shows the complete design matrixes together with both the response values obtained from the experimental work. Run 15–20 at the center point were conducted to determine the experimental error and the reproducibility of the data. RBBR removal and activated carbon yield were found to range from 30.54 to 83.56% and 11.38 to 26.59%, respectively. According to the sequential model sum of squares, the models were selected based on the highest order polynomials where the additional terms were significant and the models were not aliased. For response of RBBR removal the quadratic model was selected as suggested by the software. On the other hand, for activated carbon yield, the two-factor interaction (2FI) model was the best model to correlate the data to the response. The final empirical formula models for the RBBR removal (Y_1) and MP activated carbon yield (Y_2) in terms of coded factors after excluding the insignificant terms are represented by Eq. (6) and (7), respectively.

$$Y_1 = 77.37 + 9.70x_1 + 1.01x_2 + 15.36x_3 - 8.64x_1^2 - 3.81x_2^2 - 8.02x_3^2 - 0.16x_1x_2 + 4.91x_1x_3 + 0.025x_2x_3 \quad (6)$$

$$Y_2 = 20.45 - 2.56x_1 - 1.97x_2 - 1.89x_3 - 1.88x_1x_2 + 0.97x_1x_3 + 0.18\,x_2x_3 \quad (7)$$

The coefficient with one factor represent the effect of the particular factor, while the coefficients with two factors and those with

Table 3
Analysis of variance (ANOVA) for response surface quadratic model for RBBR removal of MP activated carbon.

Source	Sum of squares	Degree of freedom (DF)	Mean square	*F*-value	Prob. > *F*	Comment
Model	6611.48	9	734.61	18.54	<0.0001	Significant
x_1	1284.16	1	1284.16	32.41	0.0002	
x_2	13.83	1	13.83	0.35	0.5678	
x_3	3221.35	1	3221.35	81.29	<0.0001	
x_1^2	1074.97	1	1074.97	27.13	0.0004	
x_2^2	209.27	1	209.27	5.28	0.0444	
x_3^2	926.47	1	926.47	23.38	0.0007	
x_1x_2	0.20	1	0.20	0.005	0.9441	
x_1x_3	192.67	1	192.67	4.86	0.0520	
x_2x_3	0.005	1	0.005	0.0001	0.9913	
Residual	396.26	10	39.63	–	–	
Lack-of fit	394.58	5	78.92	236.13	<0.0001	Significant
Pure error	1.67	5	0.33	–	–	

second-order terms represent the interaction between two factors and quadratic effect, respectively. The positive sign in front of the terms indicates synergistic effect, whereas negative sign indicates antagonistic effect. The quality of the models developed was evaluated based on the correlation coefficients, R^2 value. In fact, the models developed seems to be the best at low standard deviation and high R^2 statistics which is closer to unity as it will give predicted value closer to the actual value for the responses [19].

In this experiment, the R^2 values for Eq. (6) and (7) were 0.943 and 0.831, respectively. This indicated that 94.3 and 83.1% of the total variation in the RBBR removal and carbon yield, respectively were attributed to the experimental variables studied. The standard deviations for the two models were 6.29 and 1.89 for Eq. (6) and (7), respectively. The R^2 values of 0.943 for Eq. (6) was considered relatively high, indicating that the predicted values for RBBR removal of the MP activated carbon would be more accurate and closer to its actual value. The R^2 of 0.831 for Eq. (7) was considered as moderate to validate the fit, which might lead to larger variation in the MP activated carbon yield predicted from the model. However, the standard deviation for this model is lower than the model for RBBR removal which indicates that the predicted values for this model is still considered as suitable to correlate the experimental data.

3.2. Analysis of variance

The significance and adequacy of the models were further justified through analysis of variance (ANOVA). In the ANOVA, the mean squares were obtained by dividing the sum of the squares of each of the variation sources, the model and the error variance, by the respective degrees of freedom. The fishers variance ratio *F*-value = (Sr^2/Se^2) is the ratio of the mean square owing to regression to the mean square owing to error. It is the measure of variation in the data about the mean. The ANOVA of the regression model demonstrates that the model is highly significant as evident from the calculated *F*-value and a very low probability value. If the value of Prob. > *F* less than 0.05, the model terms are considered as significant [21]. The ANOVA for the quadratic model for RBBR removal of MP activated carbon is listed in Table 3. The model *F*-value of 18.54 and Prob. > *F* of less than 0.0001 implied that this model was significant. In this cases, x_1, x_3, x_1^2 and x_3^2 factors were significant model terms whereas x_2, x_2^2, x_1x_2, x_1x_3 and x_2x_3 were insignificant to the response.

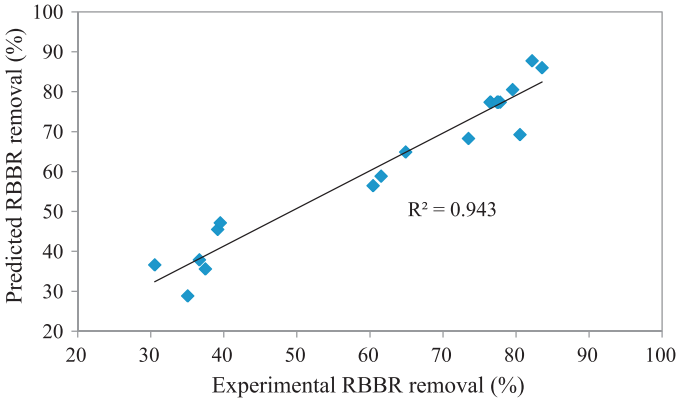

Fig. 2. Predicted versus experimental RBBR removal of MP activated carbons.

From the ANOVA for two-factor interaction model for MP activated carbon yield as shown in Table 4, the model *F*-value of 10.66 and Prob. > *F* of 0.0002 revealed that the model was significant. In this case, x_1, x_2, x_3 and x_1x_2 were significant model terms whereas x_1x_3 and x_2x_3 were insignificant to the response. From the statistical results obtained, it was shown that the above models (Eqs. (6) and (7)) were adequate to predict the RBBR removal and the activated carbon yield within the range of variables studied. In addition, Figs. 2 and 3 show the predicted values versus the experimental values for RBBR removal and carbon yield, respectively. It can be seen that the models developed were successful in capturing the correlation between the MP activated carbon preparation variables to the responses when the predicted values obtained were quite close to the experimental values.

Table 4
Analysis of variance (ANOVA) for response surface 2FI model for MP activated carbon yield.

Source	Sum of squares	Degree of freedom (DF)	Mean square	*F*-value	Prob. > *F*	Comment
Model	227.50	6	37.92	10.66	0.0002	Significant
x_1	89.44	1	89.44	25.14	0.0002	
x_2	52.93	1	52.93	14.88	0.0020	
x_3	49.02	1	49.02	13.78	0.0026	
x_1x_2	28.31	1	28.31	7.96	0.0144	
x_1x_3	7.55	1	7.55	2.12	0.1690	
x_2x_3	0.25	1	0.25	0.070	0.7957	
Residual	46.25	13	3.56	–	–	
Lack-of fit	44.81	8	5.60	19.45	0.0023	Significant
Pure error	1.44	5	0.29	–	–	

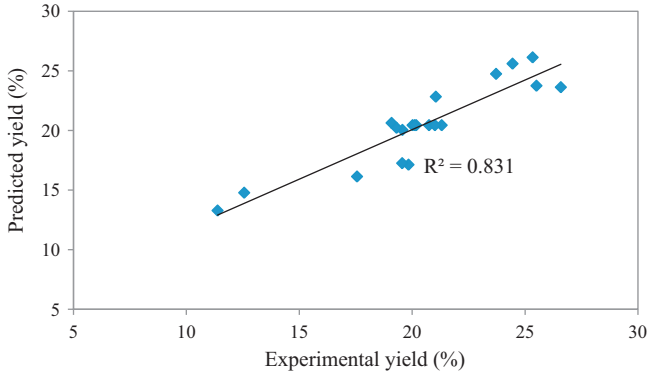

Fig. 3. Predicted versus experimental MP activated carbon yield.

As a special diagnostic test for adequacy of a model, lack-of-fit present the model performance as compared to pure error which is based on the replicate measurements [23]. *F*-value for lack of fit is calculated as the ratio between the lack-of-fit mean square and the pure error mean square. As the statistic parameter, the *F*-value is used to determine whether the lack of fit is significant or not, at a significant level α [19]. For RBBR removal, the lack-of-fit *F*-value of 236.13 implies the lack-of-fit is significant (Table 3). There is only a 0.01% chance that a "lack of fit *F*-value" this large could occur due to noise. For the carbon yield, the "lack of fit *F*-value" of 19.45 implies the lack-of-fit is undesirable significant relative to the pure error (Table 4). There is a 0.23% chance that a "lack-of-fit *F*-value" this large could occur due to noise.

3.3. RBBR removal

Based on the *F*-value as shown in Table 3, both the activation temperature and IR were found to have significant effects on the RBBR removal of MP activated carbon, whereas activation time showed the least significant effect on this response. Among all the factors being considered, IR was found to impose the greatest effect on the RBBR removal, as it showed the highest *F*-value. Besides, the quadratic effects of IR and activation temperature as well as the interaction effects between these two variables were considered moderate. Fig. 4 shows the three-dimensional response surfaces which was constructed to show the interaction effects of the activation temperature and IR on the RBBR removal. For this plot, the activation time was fixed at zero level (t = 2 h). As can be seen from Fig. 4, the RBBR removal generally increased with increase in the

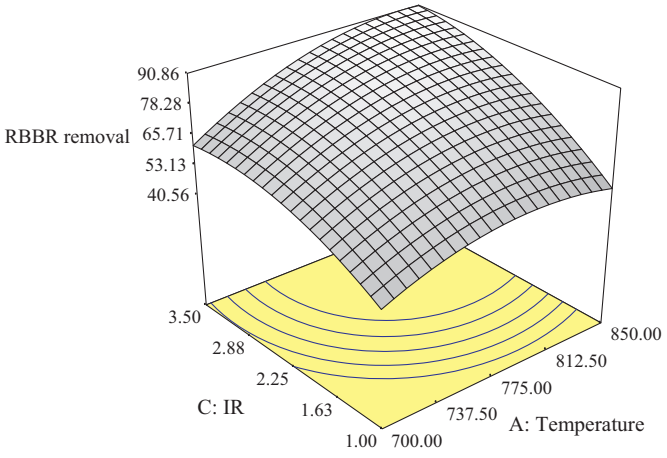

Fig. 4. Three-dimensional response surface plot of RBBR removal (effect of activation temperature and IR, t = 2 h) of MP activated carbons.

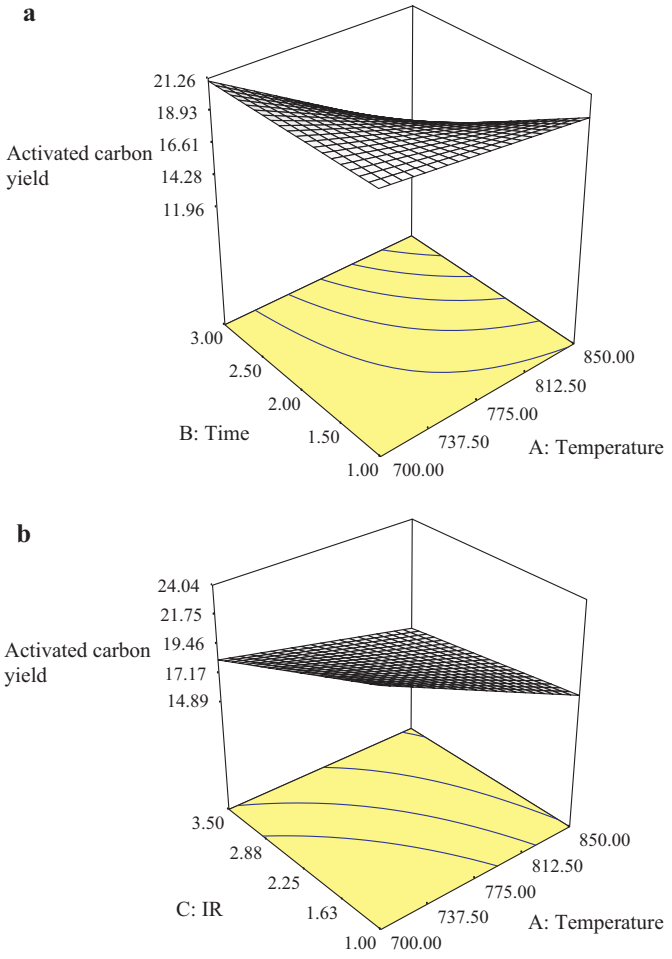

Fig. 5. Three-dimensional response surface plot of MP activated carbon yield; (a) effect of activation temperature and activation time, IR = 2.25, (b) effect of activation temperature and IR, t = 2 h.

two variables studied. The results obtained were in aggrement with the work done by Sudaryanto et al. [24] which reported that IR and activation temperature gave significant effect on the pore structure of activated carbon produced from casava peel, compared to activation time. Sentorun-Shalaby et al. [25] also found that activation time did not show much effect on the surface area obtained for activated carbons prepared from apricot stones using steam activation. Increasing in activation temperature and time would entail an opening an enlargement of the pores, which enhanced the adsorption of dye [26]. However, Gratuito et al. [27] indicated that it is not necessary to prolong activation time so much beyond the basic requirement. As doing so would cause pores enlargement, which may be undesireable depending on the requirement of a specific activated carbon application.

As the most prominent factor on RBBR removal of MP activated carbon, IR played a crucial role in the formation of pores and increase the surface area as well. This phenomena is probably due to the fact that upon the impregnation of carbons with KOH, K_2CO_3 is formed with a simultaneous evolution of CO_2 and CO [28]. In addition, activation temperature above 700 °C is believed to be responsible for the drastic expansion of the carbon material and the creation of larger surface area and high porosity due to the intercalation of metallic potassium [29], leading towards high RBBR removal efficiency. Tan et al. [14] have found that KOH could accelerate the reaction rate and therefore the quantity of pores on the activated carbon derived from coconut husk is increased correspondingly. However, El-Hendawy [30] has observed that at too

Table 5
Model validation.

Model desirability	Activation temperature, x_1 (°C)	Activation time, x_2 (h)	IR, x_3	RBBR removal (%)			Activated carbon yield (%)		
				Predicted	Experimental	Error (%)	Predicted	Experimental	Error (%)
0.800	828	1.0	3.0	83.56	80.35	3.84	21.11	20.76	1.69

high concentration of KOH, might lead to the presence of K_2CO_3 and metallic potassium that was left in the carbon and cannot easily leached even after repeated washing. This may cause blocking of some pores leading to the observed drastic decrease in the accessible area for nitrogen molecules that finally reduced the surface area of the activated carbon prepared.

3.4. Activated carbon yield

Referring to Table 4, all the three variables were found to be significant on the response for activated carbon yield, with activation temperature imposing the greatest effect on it, while activation time and IR showed almost similar effect on this response, which were considered moderate. However, the interaction effects between the variables were all less significants. Fig. 5(a) and (b) shows the three-dimensional response surface which were constructed to show the effects of activated carbon preparation variables on the MP activated carbon yield. Fig. 5(a) illustrates the effect of activation temperature and activation time on the MP activated carbon yield, with IR fixed at zero level (IR = 2.25), whereas Fig. 5(b) illustrates the effect of activation temperature and IR on the response, with activation time fixed at zero level (t = 2 h).

The carbon yield was found to decrease with increasing activation temperature, activation time and IR. From both figures, it can be seen that activation temperature was more influential factor on the MP activated carbon yield as compared to the other two variables. The highest yield was obtained when all the variables were at the minimum point within the range studied. This result was in agreement with the work done by Ahmad et al. [19] which found that activation temperature play an important role on the yield of activated carbon prepared by rattan sawdust whereas activation time did not show much effect on the carbon yield. Overall weight loss was found to increase with increasing temperature, resulting in decreasing yield of activated carbon at high temperature [21]. The weight loss was due to devolatilization of the precursors, primary to increase of the pore development and create new pores, as a result of intensifying dehydration and elimination reactions [29]. As temperature increasing, C–KOH and C–CO_2 reaction rate is increased as well, leading towards decreasing of carbon yield [26]. The effect of IR on yield of activated carbon is shown in Fig. 5(b) where increasing IR decreased the carbon yield and increased the carbon burn-off. At higher IR, the weight loss of carbon increases due to the oxidation process on the surface of carbon atoms that promote by KOH [24]. Shevkoplyas and Saranchuk [31] observed that impregnation of coal with KOH leads to the breaking of C–O–C and C–C bonds, facilitating coal decomposition during pyrolisis and as a result decreasing the carbon yield [21].

3.5. Process optimization

One of the main aims of this study was to find the optimum process parameters which activated carbons produced should have a high carbon yield and a high RBBR removal. However, it is difficult to optimize both these responses under the same condition

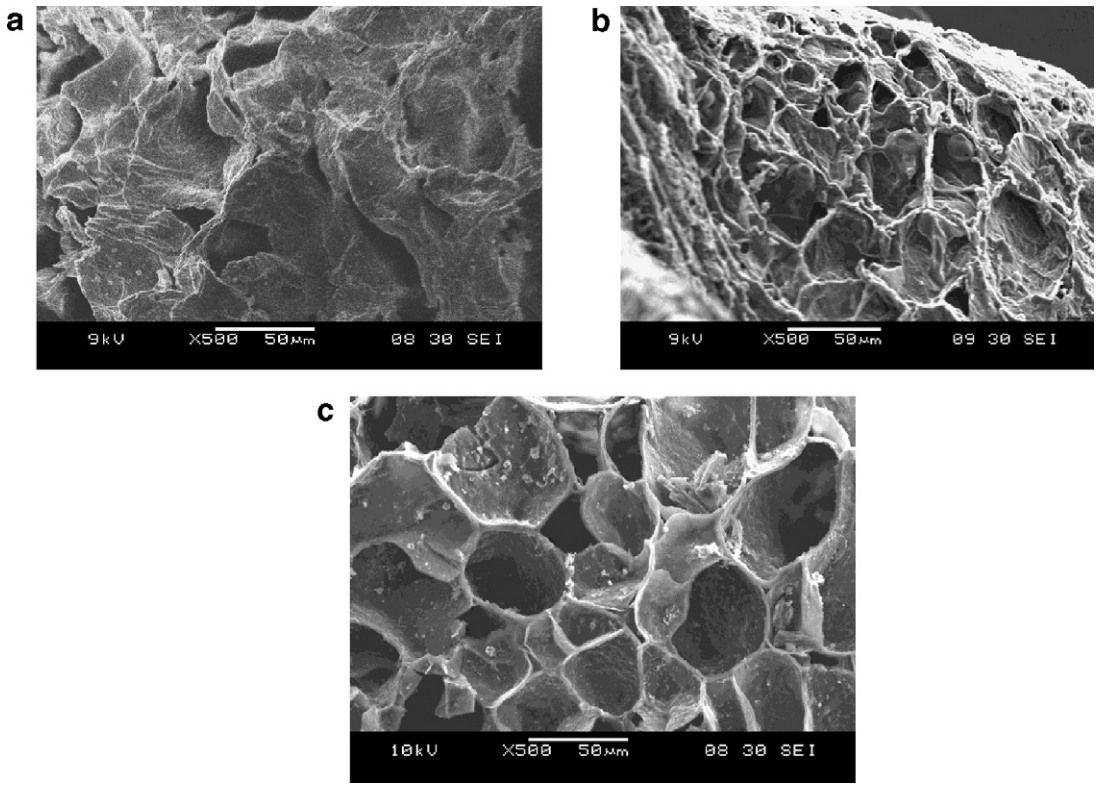

Fig. 6. Scanning electron micrographs; (a) precursor, (b) char, (c) MP activated carbon (magnifications: 500×).

Table 6
Proximate analysis and elemental contents.

Sample	Proximate analysis (%)				Elemental analysis (%)			
	Moisture	Volatile	Fixed Carbon	Ash	C	H	S	(N + O)[a]
Precursor	9.49	60.13	28.48	1.90	43.87	5.45	0.46	50.22
Char	8.42	17.44	70.45	3.69	70.84	2.54	0.20	26.82
MP activated carbon	9.08	16.36	72.93	1.63	73.10	1.27	0.08	25.55

[a] Estimated by difference.

because the interest region of factors is different. When adsorption performance increases, carbon yield will decrease and vice versa. Therefore, the function of desirability was applied using Design-Expert software version 6.0.6 (STAT-EASE Inc., Minneapolis, USA) in order to compromise between these two responses.

In the optimization analysis, the target criteria was set as maximum values for the two responses of RBBR removal (Y_1) and activated carbon yield (Y_2) while the values of the three variables were set in the ranges being studied. The experimental conditions with the highest desirability were selected to be verified. The predicted and experimental results of RBBR removal and carbon yield obtained at optimum conditions are listed in Table 5. The optimum MP activated carbon was obtained by using activation temperature, activation time and IR of 828 °C, 1 h and 3.0, respectively. The optimum activated carbon showed RBBR removal of 71.35% and activated carbon yield of 20.76%. It was observed that the experimental values obtained were in good agreement with the values predicted from the models, with relatively small errors between the predicted and the actual values, which was only 3.84% and 1.69%, for RBBR removal and activated carbon yield, respectively.

3.6. Characterization of activated carbon prepared under optimum condition

3.6.1. BET surface area and pore volume

The BET surface area, total pore volume and average pore diameter of the prepared activated carbon were found to be 994.21 m^2/g, 0.57 cm^3/g and 2.61 nm, respectively. The average pore diameter of 2.61 nm indicates that the MP activated carbon prepared was in the mesopores region according to the IUPAC classification [32]. The physiochemical activation process has contributed to the high surface area and total pore volume of the prepared activated carbon. The activated carbon development porosity is associated with gasification reaction [15].

3.6.2. Surface morphology

Fig. 6(a), (b) and (c), respectively shows the SEM images of the precursor, char and the MP activated carbon. The precursor's surface textures were rough, uneven, undulating and very little pores were presence as observed in other biomass [14,19]. After carbonization process, some irregular holes and pores were developed and found on the surfaces of the char due to the sudden burst of the thermal expansion from pyrolysis as shown in Fig. 6(b). From Fig. 6(c), it can be seen that almost homogeneous type pores structure were distributed on the surface of the MP activated carbon. This result revealed that the combination activation process of KOH and CO_2 were effective in creating well-developed pores, resulting to large surface area activated carbon with good mesoporous structure. Similar observations were reported by other researchers in their work of preparing activated carbons from coconut shells [14], oil palm empty fruit bunch [13] and oil palm fronds [33].

3.6.3. Proximate and elemental analysis

Table 6 presents the proximate and elemental analysis of precursor, char and MP activated carbon. After undergoing carbonization and activation process, the volatile matter content of the precursors decreased significantly whereas the fixed carbon content increased in activated carbons. This might be due to pyrolytic effect at high temperature where most of the organic substances have been degraded and discharged both as gas and liquid tars leaving a material with high carbon purity. A reduction of hydrogen content to a value less than 1.5% was due to the organic molecular chains ruptured after undergoing carbonization and physiochemical activation process [33]. Besides, there is also insignificant sulfur content for MP activated carbon which similar observation was obtained by Tay et al. [34] in preparing activated carbon from waste biomass by chemical activation of K_2CO_3 and KOH.

4. Conclusions

Response surface methodology was successfully used to investigate the effects of activation temperature, activation time and IR, on the percentage removal of RBBR and yield of the activated carbon prepared. The optimum MP activated carbon preparation conditions were obtained using 828 °C activation temperature, 1 h activation time and 3.0 IR resulting in 71.35% of RBBR removal and 20.76% of carbon yield. Through analysis of the response surface, activation temperature and IR were found to have significant effects on RBBR removal. Activation temperature was found to have the greatest effect on carbon yield. The MP activated carbon prepared demonstrated high surface area and well-developed porosity. MP activated carbon was shown to be a promising adsorbent for removal of Remazol Brilliant Blue R from aqueous solutions.

Acknowledgement

The authors gratefully acknowledge the financial support received in the form of research grants (PJKIMIA/814003 and PJAWAM/814021) from Universiti Sains Malaysia.

References

[1] O. Tunc, H. Tanac, Z. Aksu, Potential use of cotton plant wastes for the removal of Remazol Black B reactive dye, J. Hazard. Mater. 163 (2009) 187–198.
[2] Z. Aksu, I.A. Isoglu, Use of agricultural waste sugar beet pulp for the removal of Gemazol turquoise blue-G reactive dye from aqueous solution, J. Hazard. Mater. 137 (2006) 418–430.
[3] A. Demirbas, Agricultural based activated carbons for the removal of dyes from aqueous solutions: a review, J. Hazard. Mater. 167 (2009) 1–9.
[4] Y. Al-Degs, M.A.M. Khraisheh, S.J. Allen, M.N. Ahmad, Effect of carbon surface chemistry on the removal of reactive dyes from textiles effluent, Water Res. 34 (2000) 927–935.
[5] A.W.M. Ip, J.P. Barford, G. McKay, Production and comparison of high surface area bamboo derived active carbons, Bioresour. Technol. 99 (2008) 8909–8916.
[6] P. Baskaralingam, M. Pulikesi, V. Ramamurthi, S. Sivanesan, Modified hectorites and adsorption studies of a reactive dye—technical note, Appl. Clay Sci. 37 (2007) 207–214.
[7] Z. Aksu, S. Tezer, Equilibrium and kinetic modelling of biosorption of Remazol Black B by Rhizopus arrhizus in a batch system: effect of temperature, Process Biochem. 36 (2000) 431–439.
[8] N.K. Amin, Removal of direct blue-106 dye from aqueous solution using new activated carbons developed from pomegranate peel: adsorption equilibrium and kinetics, J. Hazard. Mater. 165 (2009) 52–62.
[9] B.H. Hameed, J.M. Salman, A.L. Ahmad, Adsorption isotherm and kinetic modeling of 2,4-D pesticide on activated carbon derived from date stones, J. Hazard. Mater. 163 (2009) 121–126.

[10] S. Altenor, B. Carene, E. Emmanuel, J. Lambert, J.-J. Ehrhardt, S. Gaspard, Adsorption studies of methylene blue and phenol onto vetiver roots activated carbon prepared by chemical activation, J. Hazard. Mater. 165 (2009) 1029–1039.
[11] M.S. Balathanigaimani, W.G. Shim, K.H. Park, J.W. Lee, H. Moon, Effects of structural and surface energetic heterogeneity properties of novel corn grain-based activated carbons on dye adsorption, Micropor. Mesopor. Mater. 118 (2009) 232–238.
[12] K. Li, Z. Zheng, X. Huang, G. Zhao, J. Feng, J. Zhang, Equilibrium, kinetic and thermodynamic studies on the adsorption of 2-nitroaniline onto activated carbon prepared from cotton stalk fibre, J. Hazard. Mater. 166 (2009) 213–220.
[13] B.H. Hameed, I.A.W. Tan, A.L. Ahmad, Preparation of oil palm empty fruit bunch-based activated carbon for removal of 2,4,6-trichlorophenol: Optimization using response surface methodology, J. Hazard. Mater. 164 (2009) 1316–1324.
[14] I.A.W. Tan, A.L. Ahmad, B.H. Hameed, Optimization of preparation conditions for activated carbons from coconut husk using response surface methodology, Chem. Eng. J. 137 (2008) 462–470.
[15] A.H. Basta, V. Fierro, H. El-Saied, A. Celzard, 2-Steps KOH activation of rice straw: an efficient method for preparing high-performance activated carbons, Bioresour. Technol. 100 (2009) 3941–3947.
[16] M. Osman, A.R. Milan, Mangosteen-Garcinia mangostana L. Southampton Centre for Underutilised Crops, University of Southampton, Southampton, UK, 2006.
[17] S. Okonogi, C. Duangrat, S. Anuchpreeda, S. Tachakittirungrod, S. Chowwanapoonpohn, Comparison of antioxidant capacities and cytotoxicities of certain fruit peels, Food Chem. 103 (2007) 839–846.
[18] R. Zien, R. Suhaili, F. Earnestly, Indrawati, E. Munaf, Removal of Pb(II), Cd(II) and Co(II) from aqueous solution using Garcinia mangostana L. fruit shell, J. Hazard. Mater. 162 (2010) 43–50.
[19] A.A. Ahmad, B.H. Hameed, A.L. Ahmad, Removal of disperse dye from aqueous solution using waste-derived activated carbon: optimization study, J. Hazard. Mater. 170 (2009) 612–619.
[20] A.M.M. Vargas, C.A. Garcia, E.M. Reis, E. Lenzi, W.F. Costa, V.C. Almeida, NaOH-activated carbon from flamboyant (Delonix regia) pods: optimization of preparation conditions using central composite rotatable design, Chem. Eng. J. 162 (2010) 43–50.
[21] J.N. Sahu, J. Acharya, B.C. Meikap, Optimization of production conditions for activated carbons from Tamarind wood by zinc chloride using response surface methodology, Bioresour. Technol. 10 (2010) 1974–1982.
[22] F. Karacan, U. Ozden, S. Karacan, Optimization of manufacturing conditions for activated carbon from Turkish lignite by chemical activation using response surface methodology, Appl. Therm. Eng. 2 (2007) 1212–1218.
[23] M.Y. Noordin, V.C. Venkatesh, S. Sharif, S. Elting, A. Abdullah, Application of response surface methodology in describing the performance of coated carbide tools when turning AISI 1045 steel, J. Mater. Process. Tech. 145 (2004) 46–58.
[24] Y. Sudaryanto, S.B. Hartono, W. Irawaty, H. Hindarso, S. Ismadji, High surface area activated carbons from olive-seed waste residue, Micropor. Mesopor. Mater. 82 (2006) 79–85.
[25] C. Sentorun-Shalaby, M.G. Ucak-Astarlıoğlu, L. Artok, C. Sarıcı, Preparation and characterization of activated carbons by one-step steam pyrolysis/activation from apricot stones, Micropor. Mesopor. Mater. 88 (2006) 126–134.
[26] A.C. Lua, T. Yang, Effect of activation temperature on the textural and chemical properties of potassium hydroxide activated carbons, J. Anal. Appl. Pyrol. 76 (2004) 96–102.
[27] M.K.B. Gratuito, T. Panyathanmaporn, R.-A. Chumnanklang, N. Sirinuntawittaya, A. Dutta, Production of activated carbon from coconut shell: optimization using response surface methodology, Bioresour. Technol. 99 (2008) 4887–4895.
[28] J. Dıaz-Teran, D.M. Nevskaia, J.L. Fierro, G.A.J. Lopez-Peinado, A. Jerez, Study of chemical activation process of a lignocellulosic material with KOH by XPS and XRD, Micropor. Mesopor. Mater. 60 (2003) 173–181.
[29] D. Adinata, W.M.A. Wan Daud, M.K. Aroua, Preparation and characterization of activated carbon from palm shell by chemical activation with K_2CO_3, Bioresour. Technol. 98 (2007) 145–149.
[30] A.N.A. El-Hendawy, An insight into the KOH activation mechanism through the production of microporous activated carbon for the removal of Pb^{2+} cations, Appl. Surf. Sci. 255 (2009) 3723–3730.
[31] V.N. Shevkoplyas, V.I. Saranchuk, The impregnation effect on low and middle rank coals structure reorganization and their behavior during pyrolysis, Fuel 79 (2000) 557–565.
[32] IUPAC, IUPAC manual of symbols and terminology, Pure Appl. Chem. 31 (1972) 587.
[33] J.M. Salman, B.H. Hameed, Effect of preparation conditions of oil palm fronds activated carbon on adsorption of bentazon from aqueous solutions, J. Hazard. Mater. 175 (2010) 133–137.
[34] T. Tay, S. Ucar, S. Karagöz, Preparation and characterization of activated carbon from waste biomass, J. Hazard. Mater. 165 (2009) 481–485.